



Bayesian analysis on interactions of exotic nuclear systems

L. Yang^a, C.J. Lin^{a,b,*}, Y.X. Zhang^a, P.W. Wen^a, H.M. Jia^a, D.X. Wang^a, N.R. Ma^a, F. Yang^a, F.P. Zhong^{a,b}, S.H. Zhong^{a,b}, T.P. Luo^a

^a China Institute of Atomic Energy, P. O. Box 275(10), Beijing 102413, China

^b Department of Physics, Guangxi Normal University, Guilin 541004, China

ARTICLE INFO

Article history:

Received 10 February 2020

Received in revised form 11 April 2020

Accepted 3 June 2020

Available online 5 June 2020

Editor: D.F. Geesaman

Keywords:

Bayesian framework

Frequentist approach

Optical model potential

Exotic nuclear system

ABSTRACT

Even though the Bayesian method has been proved to be powerful in the field of nuclear physics, it has not yet been implemented to study the properties of the reaction systems with exotic nuclei, for instance, the gross feature of the phenomenological interaction potential. So far, the optical model potential was typically evaluated by the traditional frequentist approach. However, contradictive conclusions were drawn, especially on the near-threshold behavior of the imaginary potential: threshold anomaly and abnormal threshold anomaly were derived for ${}^6\text{Li}+{}^{209}\text{Bi}$ and ${}^6\text{He}+{}^{208}\text{Pb}$ even with the same elastic scattering data. In this study, we first applied the Bayesian framework to analyze the elastic scattering data of ${}^6\text{Li}+{}^{209}\text{Bi}$. It was found that the results of Bayesian statistics strongly depend on the imposed prior distributions. Therefore, the Bayesian method has to be used with extreme caution, since the improper prior knowledge could lead to completely wrong conclusions. Since the elastic scattering data is not informative enough to constrain the prior and posterior distributions, our analysis further indicates that the results from the non-constraint frequentist approach or the flat prior distribution with a reasonable physical-boundary can be employed as convincing prior knowledge of the Bayesian framework. Based on this result, we further applied the Bayesian approach to the transfer reaction ${}^{208}\text{Pb}({}^7\text{Li}, {}^6\text{He}){}^{209}\text{Bi}$, to investigate the optical potentials of the neutron halo system ${}^6\text{He}+{}^{209}\text{Bi}$ in the outgoing channel. With the proper prior distributions, the Bayesian analysis on both the ${}^6\text{Li}+{}^{209}\text{Bi}$ and ${}^6\text{He}+{}^{208}\text{Pb}$ confirm the presence of the abnormal threshold anomaly. Therefore the applicability of the dispersion relation remains in doubt.

© 2020 Published by Elsevier B.V. This is an open access article under the CC BY license (<http://creativecommons.org/licenses/by/4.0/>). Funded by SCOAP³.

1. Introduction

It was in 1920s that the dispersion relation, as a natural consequence of the causality principle, was first introduced into physics by Kramers [1] and Kronig [2] in the study of the propagation of light in refractive media. Since then it has been successfully applied in other branches of physics [3–5]. Relevant to the low energy nuclear reaction subfield, inspired by the successes in elementary particle physics, attempts were made to apply the dispersion relation in problems in direct nuclear reactions [6]. The optical model [7] is the most successful macroscopic model in the field of nuclear reaction. It describes the nuclear interactions phenomenologically, analogous to the refraction and absorption of a light wave by a medium with complex refractive index in op-

tics. Hence the optical model potential (OMP) can be expressed as $U(r) = V(r) + iW(r)$: the real part of the OMP describes the elastic scattering process in the nuclear case, while the imaginary part represents the absorption of incident flux, i.e., all the nonelastic reaction processes [8]. The process of nuclear collision is implicitly causal, i.e., the outgoing wave cannot be generated before the arrival of the incident wave. Consequently, it is considered to have the dispersion relation between the real and imaginary parts of the OMP.

It was first pointed out by Nagarajan et al. [9] in ${}^{16}\text{O}+{}^{208}\text{Pb}$ that the dispersion relation should be responsible for the “anomalous” behavior of the OMP at energies around the Coulomb barrier [10], which is known as the threshold anomaly (TA). The TA is characterized by a sharp decrease in the imaginary potential as the energy decreases towards the Coulomb barrier, vanished at the threshold energy; meanwhile, the real part shows an anomalous variation: a localized bell-shaped structure around the barrier. Subsequent studies have shown that this is a general property of optical potentials [11–14].

* Corresponding author at: China Institute of Atomic Energy, P. O. Box 275(10), Beijing 102413, China.

E-mail address: cjlin@ciae.ac.cn (C.J. Lin).

However, unusual near-threshold behavior was observed in reactions induced by weakly bound nuclei, such as ${}^6\text{Li}$ [15,16], ${}^9\text{Be}$ [17,18] and ${}^6\text{He}$ [19]. In these exotic systems, the imaginary potential continuously increases with energy decreasing below the barrier. The influence of breakup reactions was considered to be the origin of this abnormal behavior, which was hence named as the breakup threshold anomaly [20]. However, the fundamental reason is yet unclear, for instance, the soft dipole resonance rather than the breakup may play an important role in such an abnormal trend [21]. Considering this, we would like to refer to it as the abnormal threshold anomaly (ATA).

The validity of the dispersion relation in these exotic systems, however, is still controversial [11,19,22–25]. It is mainly because OMP becomes insensitive to the elastic scattering at sub-barrier energies and exhibits large uncertainties. To attack this long-standing puzzle, we proposed a novel method, i.e., the transfer reaction method, to extract the OMPs of exotic nuclear systems in the existing reaction channel [26]. With this method, the OMP of the di-neutron halo system ${}^6\text{He}+{}^{209}\text{Bi}$ was extracted down to deep sub-barrier energy, and the threshold energy was determined for the first time for an ATA system [27,28]. The result offers strong evidence that the dispersion relation does not hold for ${}^6\text{He}+{}^{209}\text{Bi}$, which may be a common phenomenon for exotic nuclear systems [11,25]. In contrast, Rodrigo and Jin re-analyzed the elastic scattering data of ${}^6\text{Li}+{}^{209}\text{Bi}$ and ${}^6\text{He}+{}^{208}\text{Pb}$ recently, by using the bootstrap method with some strong constraints imposed [29]. They concluded that there is no significant increase in the imaginary potential at energies below the Coulomb barrier, which provided the only instance so far that the TA exists in these two exotic systems. Meanwhile, the dispersion relation still works within the uncertainties.

All the discussions above were derived from the frequentist approach, which is based on the classical definition of probability as “the number of events occurs over the total number of trials, in the limit of an infinite series of equiprobable repetitions”. In practice, the χ^2 -minimization techniques stepping through parameter space are employed primarily to evaluate the uncertainty quantification. However, this approach is unsatisfactory especially for the unrepeatable situations and for the limited sequence of repetitions [30]. In the last few years, the Bayesian [31] methods are becoming increasingly popular in the field of low energy nuclear physics [32–37]. King et al. compared directly the frequentist and Bayesian approaches to evaluate uncertainties in (d, p) reactions [38]. Their results indicate that the Bayesian framework is more reliable and flexible than the frequentist approach in quantifying uncertainties on the reaction observables. Thanks to its power and simplicity, the Bayesian framework could be of great significance to help us to make a better understanding of the nuclear interactions, even though with limited experimental data. This is the goal of the present work.

2. Theoretical framework

Bayes's theorem describes the probability of an event, based on prior knowledge of conditions that might be related to the event. It is written as

$$P(x|D) = \frac{P(D|x)P(x)}{P(D)}. \quad (1)$$

The posterior distribution, $P(x|D)$, demonstrates the most likely distribution of the parameters dependent on the given data D . The probability, $P(x)$, of the model parameter x in the absence of D , is known as the prior, which summarizes our knowledge of the parameter set. The likelihood function $P(D|x)$ is then found by running the full model with parameter set x , then comparing

the model values to the corresponding experimental observations, to evaluate how well the model reproduces the data, typically through a χ^2 . $P(D)$ is the Bayesian evidence, which typically contains a sum over all possible hypotheses each weighted by their own likelihood function.

Although the Bayes's theorem is simple in principle, calculating the Bayesian evidence numerically is either computationally intractable or impossible for multi-dimension parameters in many cases [37]. In practice, the Bayesian framework often relies on the Markov chain Monte Carlo (MCMC) [39] method to sample and obtain posterior predictions from the product of the likelihood function and prior distribution. Due to the infeasibility of performing millions of full model runs, a surrogate model, i.e., an emulator, was developed to stand in for the actual computer code [40]. The emulator is constructed to interpolate effectively from the finite set of observations of the full model, then substituted for the full model for the MCMC exploration of parameter space. In the present work, a Gaussian process emulator [40,41], with the square exponential function as the covariance function, was constructed. The emulator was then trained to accurately reproduce the results of the model calculations. The hyperparameters were tuned by performing an exhaustive search over a range of potential hyperparameters using a geometric series to increment between a minimum and maximum possible hyperparameter. The Gaussian process emulator has been proved to be extremely effective and accurate [42], and the emulator error is incorporated into the calculation of the likelihood in a simplified manner. The MADAI (Modeling and Data Analysis Initiative) [43] was employed as a wrapper code for the Bayesian analysis.

For the nuclear reaction process, we mainly concern the elastic scattering and the transfer reaction to constrain the OMP parameters. The optical model and the coupled reaction channels (CRC) technique were adopted to describe the elastic scattering and the transfer reaction, respectively, with the OMP parameters as the basic inputs. The CRC model of direct reactions proceeds by constructing a model of the system wave function and solving Schrödinger's equation as accurately as possible within that model space. It is the extension of the standard coupled-channel technique to include nuclear rearrangement or transfer reactions where one or more nucleons or clusters are transferred between the projectile and target [44]. The code FRESKO [44] was used for both the optical model and CRC calculations.

3. Data analysis and results

In the present work, we took ${}^6\text{Li}+{}^{209}\text{Bi}$ as a typical example, for which contradictory conclusions were drawn from the same elastic scattering data [45]: ATA was observed by using the traditional frequentist approach [45], while TA was presented through the bootstrap analysis imposed with physical constraints [29]. To be consistent with the previous works, we only consider the Woods-Saxon volume term for both the real and imaginary potentials, with parameters V (W), r_V (r_W), a_V (a_W) for the depth, radius and diffuseness of the real (imaginary) part, respectively. The Bayesian method was used to obtain posterior distributions of the parameters with 68.3% confidence intervals, which is consistent with the previous frequentist analysis. 1000 parameter sets were chosen from the prior parameter space according to Latin hypercube sampling technique. These parameters were then used as the input of the optical model calculations and the results were used to train the emulator. After the finish of the emulator tuning, MCMC procedure was performed one million times to generate a sampling of the posterior distribution, with 10000 samples discarded at the beginning of the MCMC run (burn-in samples).

Two sets of Gaussian priors were chosen: one is centered at the OMP parameters from Ref. [45] leading to the ATA phe-

Table 1

Initial and final adopted geometric parameters of OMP for ${}^6\text{Li}+{}^{209}\text{Bi}$ for different approaches, in the unit of fm. The initial parameters of the Gaussian distributions are listed as (mean, width). While for the flat prior, the ranges of the initial parameters are presented.

	Initial values				Fixed values			
	r_V	a_V	r_W	a_W	r_V	a_V	r_W	a_W
TA prior ^a	1.38, 0.69	0.78, 0.39	1.45, 0.73	0.50, 0.25	1.30	0.83	1.45	0.54
ATA prior ^b	-	-	1.2, 0.6	$\sim 0.75, 0.38$	1.05	0.69	1.16	0.70
flat prior	0.5-2.0	0.2-2.0	0.5-2.0	0.2-2.0	1.03	0.61	1.21	0.82

^a The initial values are taken from the Bootstrap analysis with constraints, leading to the TA conclusion [29].

^b The initial values are taken from the traditional frequentist analysis with the microscopic double-folded potential (DFP) for the real part, which leads to the ATA conclusion [45].

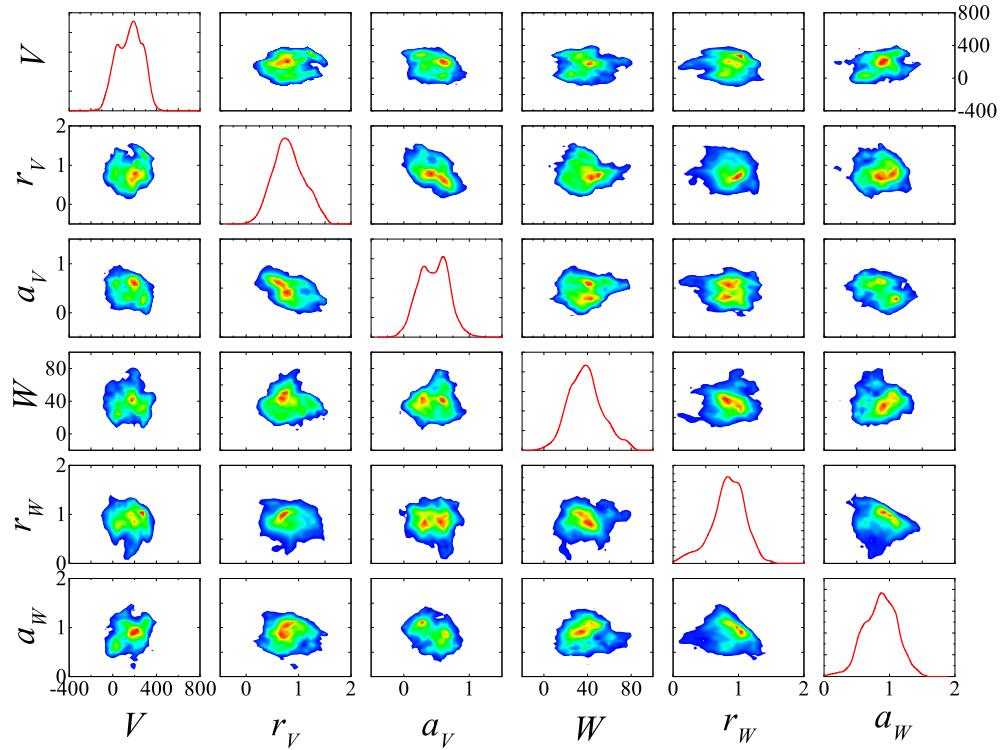


Fig. 1. Two-dimensional marginal posterior distributions for the parameters (diagonal) and scatter plots for the correlations between parameters for ${}^6\text{Li}+{}^{209}\text{Bi}$ at 26 MeV with the ATA prior. Depths (V , W) are in MeV and radii (r_V , r_W) and diffuseness (a_V , a_W) are in fm.

nomenon, while the other is centered at the parameters from Ref. [29] leading to the TA phenomenon. Therefore, we refer to these two sets as the ATA and TA priors, respectively. As a comparison, the Bayesian analysis with a flat prior within a bounded space was also performed. In a first step, all the six parameters were searched within a wide window: the widths of Gaussian priors distribution were fixed as 50% of the initial values, while for the flat prior, the parameter ranges were set as 0-500 and 0-100 MeV for the real and imaginary depths, respectively. The geometric parameters (centers and widths of the Gaussian priors as well as ranges of the flat prior) are listed in Table 1, in the “Initial values” columns. As an example, Fig. 1 shows the posterior distributions for the parameters and the correlation between them at $E_{\text{lab}} = 26$ MeV with the ATA prior. Similar results were obtained with other priors, but not shown here. In a second step, the geometric parameters were fixed at the weighted mean values derived from the first step analysis, as listed in the “Fixed values” columns of Table 1, leaving only the potential depths to be searched within a narrower window, which is about one standard deviation. As listed in Table 1, it can be seen that the Bayesian analysis with TA prior deduced similar parameters to the bootstrap analysis in Ref. [29]. However, these parameters

are different from the Bayesian analysis with ATA and flat priors, which are consistent with the results of the double-folded model [45].

It is known that the OMP parameters can only be determined unambiguously in the vicinity of the sensitive radius, R_s , which is established before any substantial overlap of the two nuclear matter distributions [14,46]. The energy dependence of potential depths obtained from different priors at $R_s=12.40$ fm [45] is presented in Fig. 2, along with the frequentist results taken from Refs. [29] and [45] marked by the corresponding hollow symbols. Two distinct trends are observed as denoted by the shadow regions in Fig. 2: the ATA and flat priors lead to the ATA phenomenon, while TA is observed with the TA prior distribution. However, despite the significant difference between the OMP parameters, all of these parameter sets can reproduce the experimental elastic scattering data properly, as shown in Fig. 3, where only the Bayesian results of the present work are presented.

It is obvious that the final inference strongly depends on the prior choice, which has been regarded historically as the problem of the Bayesian framework [30]. The prior choice ought to reflect as accurately as possible the knowledge about the problem in question. However, the optical model, as a phenomenological model,

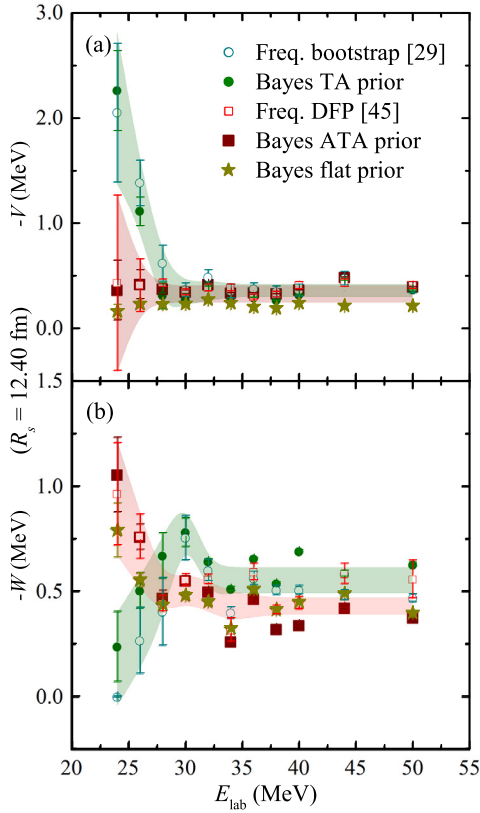


Fig. 2. Energy dependence of the real (a) and imaginary (b) potentials at the sensitivity radius of 12.40 fm for the ${}^6\text{Li}+{}^{209}\text{Bi}$ system. Full squares, circles, and stars denote the Bayesian results with ATA prior, TA prior and flat prior respectively. Hollow squares and circles represent the frequentist results taken from Refs. [45] and [29], respectively. Error bars represent 68.3% confidence intervals derived by Bayesian analysis. Shadow regions are used to guide the eyes.

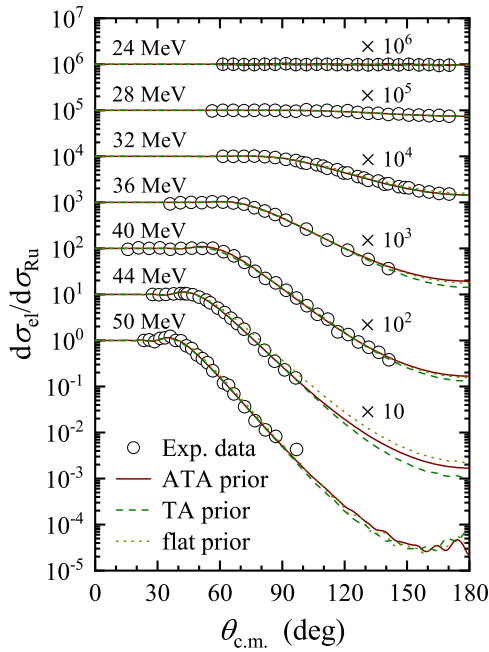


Fig. 3. Angular distributions of elastic scattering for ${}^6\text{Li}+{}^{209}\text{Bi}$ at some typical energies. Circles are the experimental data taken from Ref. [45]. Solid, dashed and dotted curves denote the optical model calculation results with the OMP parameters obtained from Bayesian approaches with ATA, TA and flat prior distributions, respectively.

has ambiguity, and the potential parameters become insensitive to the elastic scattering data especially in the sub-barrier region because of the strong Coulomb repulsion. This can be demonstrated clearly by Fig. 3, where similar optical model outputs are derived with significantly different OMP parameters. Therefore, the elastic scattering data are not informative enough to constrain the prior. Under this circumstance, the flat prior is often a standard choice, with the rationale that we should assign equal probability to equal states of knowledge [30]. For the frequentist analysis in Ref. [29], a constraint of “the strength at energies below the Coulomb barrier being small compared to the strength at higher energies” was imposed in the bootstrap approach, which is actually a TA constraint on the OMP parameters. Therefore, it is not surprising that the authors drew the TA conclusion for the exotic nuclear systems. However, for the frequentist approach employed in Ref. [45], the parameters were searched in the “full” parameter space without any constraint, which is equivalent to introduce a flat prior within a physically bounded space to the Bayesian framework. Considering the uninformative elastic scattering data, it is a more convincing way to apply the Bayesian approach with the results derived from the non-constraint frequentist analysis or with a flat prior within a physically bounded space.

Based on the above discussion, we further applied the Bayesian approach to study the OMP of the neutron-halo ${}^6\text{He}+{}^{209}\text{Bi}$ system, with the elastic scattering data [19] and the transfer reaction data ${}^{208}\text{Pb}({}^7\text{Li}, {}^6\text{He}){}^{209}\text{Bi}$ [27,28,47]. To simplify the procedure, we only consider the depth parameters, with the geometric parameters fixed as the previous frequentist results. Gaussian priors centered at the potential depths derived from the previous works were introduced. The optical model and CRC calculations were performed to train the emulator for the elastic scattering and transfer reaction analysis, respectively. In the CRC calculation, we considered the couplings from the ${}^7\text{Li}+{}^{208}\text{Pb}$ inelastic scattering to the first three excited states of ${}^7\text{Li}$ and the reorientations of these states, with the adoption of the postrepresentation and the full complex remnant term. The details of the coupling scheme, as well as the OMP parameters of the entrance channel were described in Refs. [27,28,47]. The energy dependence of the real and imaginary potentials at $R_s=13.50$ fm is shown in Fig. 4, together with the frequentist results.

It can be seen in Fig. 4 that the results derived from the elastic scattering data present very large uncertainties, especially in the sub-barrier region. That is mainly because of the limitations of the intensity and/or the phase-space qualities of radioactive ion beams. For the transfer reaction method, thanks to the usage of a high-quality stable beam and the constraint from the fulfillment of the nucleon transfer process, the much more precise OMP can be extracted. Therefore, the following discussions are based only on the results with transfer reaction data. Compared with the results derived from the frequentist approach, the Bayesian produces smaller uncertainties, especially for the imaginary potentials at sub-barrier energies. It further demonstrates the power of Bayesian statistics in uncertainty quantification. According to the extrapolation of the Bayesian analysis, the threshold energy can be determined as 13.70 ± 0.54 MeV, which is consistent with that of the previous work, 13.73 ± 1.63 MeV [27]. Moreover, the calculation result for the real potential according to the dispersion relation with the variation of the imaginary part is shown by the solid curve in Fig. 4 (a), where the linear schematic model [11] was employed to fit the imaginary potential as the solid curves shown in Fig. 4 (b). Same as the results from the frequentist approach, as shown by the dashed lines, it again indicates that the dispersion relation does not hold for ${}^6\text{He}+{}^{209}\text{Bi}$. As well known that the dispersion relation results from the causality principle, thus any wave/particle should follow this relation when it passes through a medium. Considering its importance, it would be desirable to investigate the validity of

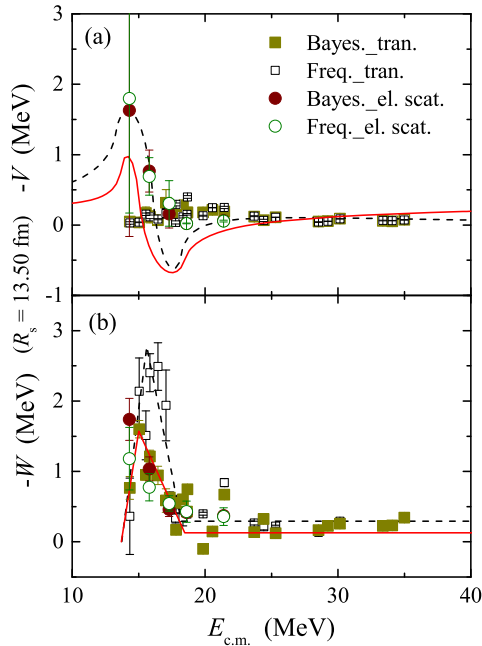


Fig. 4. Energy dependence of the real (a) and imaginary (b) potentials at the sensitivity radius of 13.50 fm for the ${}^6\text{He}+{}^{209}\text{Bi}$ system. Full and hollow squares represent the results from Bayesian and frequentist approaches with transfer reaction data [27], respectively. Same as the square symbols, but circles for the results of elastic scattering data [19]. The solid and dashed curves in (b) show the linear segment fitting for the imaginary potentials derived from Bayesian and frequentist methods with transfer reaction data. The prediction of the dispersion relation according to the variation of the imaginary potentials are shown in (a) by the corresponding curves. Error bars represent 68.3% confidence intervals.

the dispersion relation in a wide range of exotic nuclear systems, which may have significant implications on other areas of knowledge.

4. Summary and conclusions

In summary, we applied the Bayesian approach for the first time to study the properties of OMPs of exotic nuclear systems. We found that the observed energy dependence of OMP parameters strongly depends on the prior knowledge imposed in the Bayesian framework. Improper prior knowledge could lead to the wrong conclusion. Thus the application of the Bayesian approach must be with extreme caution in data analysis, i.e., with the proper prior distribution, not only for nuclear physics but also for other subfields. Relevant to our subfield, if we use TA derived from tightly bound nuclear systems as the prior distribution, we then cannot obtain the unusual near-threshold behavior for the exotic nuclear systems, which reveals the actual reaction dynamics and underlying physics. Considering the elastic scattering data is not informative enough to constrain the prior and posterior distributions, we suggest that the results from the non-constraint frequentist approach or a flat distribution could be employed as a convincing prior knowledge of the Bayesian framework. Based on this result, we further applied the Bayesian method in the transfer reaction to investigate the OMP behavior of the neutron-halo system ${}^6\text{He}+{}^{209}\text{Bi}$. The abnormal near-threshold behavior and the inapplicability of the dispersion relation were confirmed, as the previous frequentist analysis concluded. The transfer reaction method combining with Bayesian statistics with proper prior distributions offers an attractive approach to investigate the nuclear potential, especially in the sub-barrier region. It is desirable to further apply this approach to explore the properties of the interactions of exotic nuclear systems.

Declaration of competing interest

The authors declare that they have no known competing financial interests or personal relationships that could have appeared to influence the work reported in this paper.

Acknowledgements

This work is supported by the National Key R&D Program of China (Contract No. 2018YFA0404404), the National Natural Science Foundation of China (Grants Nos. 11635015, U1732145, 11705285, U1867212, 11805280, and 11961131012), and the Continuous Basic Scientific Research Project (No. WDJC-2019-13).

References

- [1] H.A. Kramers, *Atti. Congr. Int. Fis., Como 2* (1927) 545.
- [2] R. Kronig, *J. Opt. Soc. Am.* 12 (1926) 547.
- [3] J.S. Toll, *Phys. Rev.* 104 (1956) 1760.
- [4] S. Mandelstam, *Rep. Prog. Phys.* 25 (1962) 99.
- [5] M. Gell-Mann, M.L. Goldberger, W. Thirring, *Phys. Rev.* 95 (1954) 1612.
- [6] H.J. Schnitzer, *Rev. Mod. Phys.* 37 (1965) 666.
- [7] S. Fernbach, R. Serber, T.B. Taylor, *Phys. Rev.* 75 (1949) 1352.
- [8] P.E. Hodgson, *Rep. Prog. Phys.* 34 (1971) 765.
- [9] M.A. Nagarajan, C.C. Mahaux, G.R. Satchler, *Phys. Rev. Lett.* 54 (1985) 1136.
- [10] J.S. Lilley, B.R. Fulton, M.A. Nagarajan, I.J. Thompson, D.W. Banes, *Phys. Lett. B* 151 (1985) 181.
- [11] C. Mahaux, H. Ngô, G.R. Satchler, *Nucl. Phys. A* 449 (1986) 354.
- [12] G.R. Satchler, *Phys. Rep.* 199 (1991) 147.
- [13] M.E. Brandan, G.R. Satchler, *Phys. Rep.* 285 (1997) 143.
- [14] C.J. Lin, J.C. Xu, H.Q. Zhang, Z.H. Liu, F. Yang, L.X. Lu, *Phys. Rev. C* 63 (2001) 064606.
- [15] N. Keeley, S.J. Bennett, N.M. Clarke, et al., *Nucl. Phys. A* 571 (1994) 326.
- [16] Zhang Chun-Lei, Zhang Huan-Qiao, Lin Cheng-Jian, et al., *Chin. Phys. Lett.* 23 (2006) 1146.
- [17] C. Signorini, A. Andrighetto, M. Ruan, J.Y. Guo, L. Stroe, F. Soramel, et al., *Phys. Rev. C* 61 (2000) 061603(R).
- [18] N. Yu, H.Q. Zhang, H.M. Jia, et al., *J. Phys. G* 37 (2010) 075108.
- [19] A.R. Garcia, J. Lubian, I. Padron, P.R.S. Gomes, T. Lacerda, V.N. Garcia, A. Gomez Camacho, E.F. Aguilera, *Phys. Rev. C* 76 (2007) 067603.
- [20] M.S. Hussein, P.R.S. Gomes, J. Lubian, L.C. Chamon, *Phys. Rev. C* 73 (2006) 044610.
- [21] S. Nakayama, T. Yamagata, H. Akimune, et al., *Phys. Rev. Lett.* 85 (2000) 262.
- [22] A. Pakou, N. Alamanos, A. Lagoyannis, et al., *Phys. Lett. B* 556 (2003) 21.
- [23] F. Tprabi, E.F. Aguilera, O.N. Ghodsi, A. Gómez-Camacho, *Nucl. Phys. A* 994 (2020) 121661.
- [24] K. Zerva, A. Pakou, N. Patronis, et al., *Eur. Phys. J. A* 48 (2012) 102.
- [25] R. Lipperheide, A. Schmidt, *Nucl. Phys. A* 112 (1968) 65.
- [26] C.J. Lin, F. Yang, P. Zhou, et al., *AIP Conf. Proc.* 853 (2006) 81.
- [27] L. Yang, C.J. Lin, H.M. Jia, et al., *Phys. Rev. Lett.* 119 (2017) 042503.
- [28] L. Yang, C.J. Lin, H.M. Jia, et al., *Phys. Rev. C* 96 (2017) 044615.
- [29] Rodrigo Navarro Pérez, Jin Lei, *Phys. Lett. B* 795 (2019) 200.
- [30] Roberto Trotta, *Contemp. Phys.* 49 (2008) 71.
- [31] M. Bayes, M. Price, *Philos. Trans.* 53 (1763) 370.
- [32] R.J. Furnstahl, N. Klco, D.R. Phillips, S. Wesolowski, *Phys. Rev. C* 92 (2015) 024005.
- [33] J.A. Melendez, S. Wesolowski, R.J. Furnstahl, *Phys. Rev. C* 96 (2017) 024003.
- [34] L. Neufcourt, Y. Cao, W. Nazarewicz, F. Viens, *Phys. Rev. C* 98 (2018) 034318.
- [35] R. Orford, N. Vassh, J.A. Clark, G.C. McLaughlin, M.R. Mumpower, G. Savard, et al., *Phys. Rev. Lett.* 120 (2018) 262702.
- [36] Y. Lim, J.W. Holt, *Phys. Rev. Lett.* 121 (2018) 062701.
- [37] A.E. Lovell, F.M. Nunes, *Phys. Rev. C* 97 (2018) 064612.
- [38] G.B. King, A.E. Lovell, L. Neufcourt, F.M. Nunes, *Phys. Rev. Lett.* 122 (2019) 232502.
- [39] N. Metropolis, A.W. Rosenbluth, M.N. Rosenbluth, A.H. Teller, E. Teller, *J. Chem. Phys.* 21 (1953) 1087.
- [40] F.A. Gomez, C.E. Coleman-Smith, B.W. O'Shea, J. Tumlinson, R.L. Wolpert, *Astrophys. J.* 760 (2012) 112.
- [41] A. O'Hagan, *Reliab. Eng. Syst. Saf.* 91 (2006) 1290.
- [42] J. Novak, K. Novak, S. Pratt, J. Vredevoogd, C.E. Coleman-Smith, R.L. Wolpert, *Phys. Rev. C* 89 (2014) 034917.
- [43] Available at <https://github.com/MADAI/DistributionSampling>.
- [44] I.J. Thompson, *Comput. Phys. Rep.* 7 (1988) 167.
- [45] S. Santra, S. Kailas, K. Ramachandran, V.V. Parkar, V. Jha, B.J. Roy, P. Shukla, *Phys. Rev. C* 83 (2011) 034616.
- [46] J.G. Cramer, R.M. DeVries, *Phys. Rev. C* 22 (1980) 91.
- [47] L. Yang, C.J. Lin, H.M. Jia, et al., *Phys. Rev. C* 89 (2014) 044615.